

# Probing the relaxation mechanism that interferes with polarization measurement using the C<sub>2</sub> doublet of 1,2-[<sup>13</sup>C]<sub>2</sub>-pyruvate

J. Y. Lau<sup>1,2</sup>, A. P. Chen<sup>3</sup>, J. Zhu<sup>4</sup>, G. Wu<sup>4</sup>, and C. H. Cunningham<sup>1,2</sup>

<sup>1</sup>Department of Medical Biophysics, University of Toronto, Toronto, Ontario, Canada, <sup>2</sup>Imaging Research, Sunnybrook Health Sciences Centre, Toronto, Ontario, Canada, <sup>3</sup>GE Healthcare, Toronto, Ontario, Canada, <sup>4</sup>Department of Chemistry, Queen's University, Kingston, Ontario, Canada

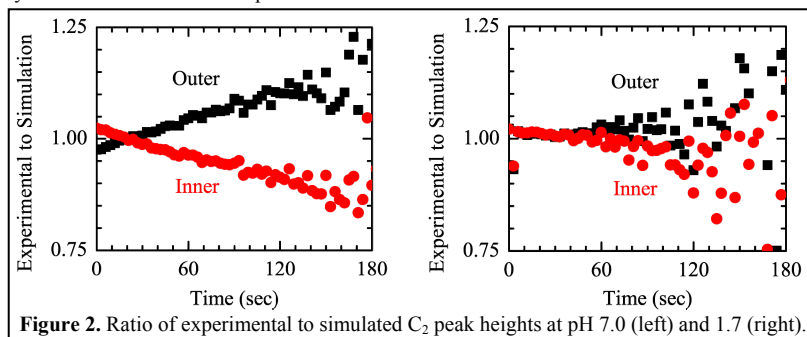
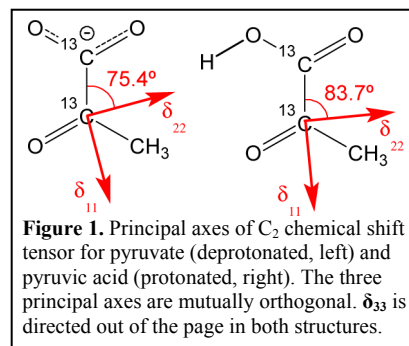
**Introduction:** Direct measurement of polarization (1-2) is of interest in pre-polarized <sup>13</sup>C studies since it would enable calculation of substrate concentration at the tissue of interest *in vivo*. Measurement of initial C<sub>1</sub> polarization using the asymmetry in the C<sub>2</sub> doublet of 1-[<sup>13</sup>C]-pyruvate has been demonstrated both *in vitro* and *in vivo* (3). With 1,2-[<sup>13</sup>C]<sub>2</sub>-pyruvate, C<sub>1</sub> polarization could, in principle, be mapped as a function of time if the C<sub>2</sub> asymmetry were followed by small tip angle excitations. However, the C<sub>2</sub> doublet has been observed to evolve beyond AB asymmetry to exhibit a reversal in relative peak heights (3). Cross correlation between the dipolar field and chemical shift anisotropy (CSA) has been shown to result in non-uniform relaxation among lines within a multiplet (4), which may resemble a reversal in relative peak heights for a doublet. The CSA at C<sub>2</sub> is expected to change with pH as the loss of symmetry upon protonation would disrupt the delocalized π-system. In this study, we examine the potential role of dipolar-CSA cross correlation in influencing C<sub>2</sub> relaxation beyond AB asymmetry.

**Methods:** Quantum chemistry: Chemical shielding tensors were computed using the Amsterdam Density Functional (version 2009.01) software package (5) in the basis set of Slater-type orbitals at the valence triple- $\zeta$  level with one polarization function (TZP). Relativistic spin orbital effects were treated with the zero order regular approximation (ZORA). The structure of pyruvate was approximated by removing the hydroxyl proton from the reported microwave structure of pyruvic acid (6). Principal axis chemical shielding values  $\sigma$  were converted to chemical shifts  $\delta$  using the relation  $\delta = 186.4 - \sigma$  (7). Polarization and spectroscopy: A solution of 15 mM OX63 trityl radicals (Oxford Instruments, Abingdon, UK) and 1 mM Gd-DOTA in 30 mg of 1,2-[<sup>13</sup>C]<sub>2</sub>-pyruvic acid (99%, Isotec, Miamisburg, OH) was polarized using a HyperSense DNP polarizer (Oxford Instruments). The polarized solid state was rapidly dissolved in a Tris-buffered NaOH/EDTA solution to give an 80 mM solution largely of the deprotonated form. The protonated form was prepared by dissolution in an analogous volume of deionized H<sub>2</sub>O (with 100 mg/L of EDTA). A syringe with ~3 mL of the polarized solution was promptly inserted into a GE MR750 3T scanner (GE Healthcare, Waukesha WI) following dissolution. Broadband <sup>13</sup>C spectra were acquired using hard pulses of 5° flip angles (TR = 3s, 10 kHz bandwidth, 4k points, NS = 96). Spectra at thermal equilibrium were acquired immediately after every hyperpolarized experiment with the addition of ~24  $\mu$ L of Magnevist to shorten the T<sub>1</sub> (90° hard pulses, 4k points, TR = 5s/10s, NS = 256/192 at pH 7.0/1.7). Spectral analysis was performed using the SAGE™ software package (GE Healthcare).

**Results and Discussion:** Chemical shift anisotropy: Principal axis components of the chemical shift tensors ( $\delta_{11}$ ,  $\delta_{22}$ ,  $\delta_{33}$ ) were calculated as (284.7, 228.9, 99.7) ppm for pyruvate and (306.7, 222.0, 101.2) ppm for pyruvic acid. The orientations of these principal axes in the molecular frame are given in Figure 1. The most significant effect of protonation is seen in the  $\delta_{11}$  principal axis component, where it increases by 22 ppm and changes in direction by 8°. Spectral analysis: 10 Hz apodization was applied to every spectrum. The instantaneous polarization was determined by multiplying the ratio of hyperpolarized to thermally polarized doublet integral by the Boltzmann population difference of 2.47 ppm. Due to the overlap between the two peaks within the doublets of C<sub>1</sub> and C<sub>2</sub>, the peak height was found to be a more accurate measure than integration for individual peak analysis. Density matrix simulations: For each time point, density matrices for C<sub>1</sub> and C<sub>2</sub> were constructed using the measured instantaneous polarizations and combined by direct tensor product. These diagonal density matrices were perturbed by a 5° tip along the x-axis and allowed to evolve under a Hamiltonian constructed using the experimental chemical shifts of C<sub>1</sub> and C<sub>2</sub> and the measured <sup>1</sup>J-coupling constant of 66 Hz. The asymmetry in the C<sub>2</sub> doublets of these simulated spectra reflects both the non-equilibrium population difference due to polarization and the intrinsic AB distortion determined by the resonant frequency difference and J-coupling constant. Comparison between experimental and simulated spectra: As the polarization decreased with T<sub>1</sub> relaxation, the simulated C<sub>2</sub> doublet simply returned to the thermal equilibrium configuration rather than exhibiting the observed reversal of relative heights. Measured and simulated T<sub>1</sub> obtained by fitting the heights of individual peaks are summarized in Table 1. Based on polarization alone, the simulation was able to reproduce the experimental T<sub>1</sub> at pH 1.7, but discrepancies at pH 7.0 suggest the existence of additional relaxation mechanisms that preferentially enhance relaxation of one peak in the doublet while proportionately retarding the relaxation of its partner. To allow comparison of peak heights, each set of simulated peak heights was scaled uniformly by a constant, as determined by the method of least squares, to place the simulated data onto the same scale as the experimental intensities. The ratio of experimental to scaled simulated peak heights should reveal any contributions from additional relaxation mechanisms as discrepancies from unity. From Figure 2, experimental and simulated peak intensities are in good agreement at early times under both conditions, which supports the validity of the selective C<sub>2</sub> excitation technique of measuring initial C<sub>1</sub> polarization (3). The rapid divergence at pH 7.0 suggests that an additional relaxation mechanism becomes dominant as polarization decreases, while the C<sub>2</sub> asymmetry remains strongly correlated with polarization at low pH. The CSA orientation in the protonated form may be less effective at coupling with the dipolar field, thereby reducing the significance of dipolar-CSA cross correlation in pyruvic acid.

**Table 1.** Measured/simulated T<sub>1</sub> (sec).

pH	C <sub>1</sub>		C <sub>2</sub>	
	Upfield	Downfield	Upfield	Downfield
7.0	57/60	66/63	44/46	51/48
1.7	31/32	35/35	28/27	31/31



**Conclusions:** It was shown that solution pH has an effect on the relaxation mechanism that currently interferes with polarization measurement using C<sub>2</sub> asymmetry of 1,2-[<sup>13</sup>C]<sub>2</sub>-pyruvate. We plan to perform analogous pH 7 experiments at 7T, where CSA relaxation can be changed via field-dependence without altering solution composition. Further simulations incorporating the CSA relaxation mechanism are required to determine whether the difference in CSA alone is sufficient to explain the behaviour at both pH. Inclusion of intermolecular interactions and electrostatic attraction to Na<sup>+</sup> in neutralized solutions may yield more accurate CSA predictions.

**Acknowledgements:** Quantum chemistry computations were carried out on Sun SPARC M9000 servers (256 × 2.5 GHz SPARC64-VII processors, 2 TB of RAM) at the High Performance Computing Virtual Laboratory (HPCVL) at Queen's University.

**References:** 1. J.H. Ardenkjaer-Larsen *et al. Proc. Natl. Acad. Sci. USA* **100**: 10158 (2003) 2. R.E. Hurd *et al. 50<sup>th</sup> ENC*, p438 3. A.P. Chen *et al. Proc. Intl. Soc. Mag. Reson. Med.* **18**: 3261 (2010) 4. V.A. Daragan and K.H. Mayo *Chem. Phys. Lett.* **206**: 393 (1993) 5. M. Krykunov, T. Ziegler, and E. van Lenthe *Int. J. Quantum Chem.* **109**: 1676 (2009) 6. Z. Zhou, D. Dongmei, and A. Fu *Vib. Spectrosc.* **23**: 181 (2000) 7. K.B. Wiberg *J. Comput. Chem.* **20**: 1299 (1999)